ISSN 1674-1056
http://cpb.iphy.ac.cn
http://iopscience.iop.org/cpb
中国物理 B
Chinese Physics
中国物理 Chinese Physics B

Off-stoichiometry indexation of $BiFeO_3$ thin film on silicon by Rutherford backscattering spectrometry

Ze-Song Wang(王泽松), Ren-Zheng Xiao(肖仁政), Chang-Wei Zou(邹长伟), Wei Xie(谢伟), Can-Xin Tian(田灿鑫), Shu-Wen Xue(薛书文), Gui-Ang Liu(刘贵昂), Neena Devi, De-Jun Fu(付德君)
Citation: Chin. Phys. B . 2018, 27(4): 047901. **doi:** 10.1088/1674-1056/27/4/047901

Journal homepage: http://cpb.iphy.ac.cn; http://iopscience.iop.org/cpb

What follows is a list of articles you may be interested in

Calculation of electric field-temperature (*E, T*) phase diagram of a ferroelectric liquid crystal near the SmA-SmC_α^* transition

F Trabelsi, H Dhaouadi, O Riahi, T Othman
Chin. Phys. B . 2018, 27(3): 037701. **doi:** 10.1088/1674-1056/27/3/037701

Field-induced phase transitions in chiral smectic liquid crystals studied by the constant current method

H Dhaouadi, R Zgueb, O Riahi, F Trabelsi, T Othman
Chin. Phys. B . 2016, 25(5): 057704. **doi:** 10.1088/1674-1056/25/5/057704

Preparation and characterization of $Sr_{0.5}Ba_{0.5}Nb_2O_6$ glass-ceramic on piezoelectric properties

Shan Jiang(姜珊), Xuan-Ming Wang(王炫明), Jia-Yu Li(李佳宇),Yong Zhang(张勇), Tao Zheng(郑涛), Jing-Wen Lv(吕景文)
Chin. Phys. B . 2016, 25(3): 037701. **doi:** 10.1088/1674-1056/25/3/037701

Ultrahigh frequency tunability of aperture-coupled microstrip antenna via electric-field tunable BST

Du Hong-Lei, Xue Qian, Gao Xiao-Yang, Yao Feng-Rui, Lu Shi-Yang, Wang Ye-Long, Liu Chun-Heng, Zhang Yong-Cheng, Lü Yue-Guang, Li Shan-Dong
Chin. Phys. B . 2015, 24(12): 127704. **doi:** 10.1088/1674-1056/24/12/127704

Temperature dependences of ferroelectricity and resistive switching behavior of epitaxial $BiFeO_3$ thin films

Lu Zeng-Xing, Song Xiao, Zhao Li-Na, Li Zhong-Wen, Lin Yuan-Bin, Zeng Min, Zhang Zhang, Lu Xu-Bing, Wu Su-Juan, Gao Xing-Sen, Yan Zhi-Bo, Liu Jun-Ming
Chin. Phys. B . 2015, 24(10): 107705. **doi:** 10.1088/1674-1056/24/10/107705

Off-stoichiometry indexation of $BiFeO_3$ thin film on silicon by Rutherford backscattering spectrometry*

Ze-Song Wang(王泽松)[1,†], Ren-Zheng Xiao(肖仁政)[2], Chang-Wei Zou(邹长伟)[1], Wei Xie(谢伟)[1], Can-Xin Tian(田灿鑫)[1], Shu-Wen Xue(薛书文)[1], Gui-Ang Liu(刘贵昂)[1], Neena Devi[3], and De-Jun Fu(付德君)[3]

[1] *School of Physics and Technology, Lingnan Normal University, Zhanjiang* 524048, *China*

[2] *College of Mechanical and Power Engineering, Three Gorges University, Yichang* 443002, *China*

[3] *Key Laboratory of Artificial Micro- and Nano-Materials of Ministry of Education of China, School of Physics and Technology, Wuhan University, Wuhan* 430072, *China*

(Received 26 September 2017; revised manuscript received 12 January 2018; published online 10 March 2018)

$BiFeO_3$ is a multiferroic material with physical properties very sensitive to its stoichiometry. $BiFeO_3$ thin films on silicon substrate are prepared by the sol–gel method combined with layer-by-layer annealing and final annealing schemes. X-ray diffraction and scanning electron microscopy are employed to probe the phase structures and surface morphologies. Using Rutherford backscattering spectrometry to quantify the nonstoichiometries of $BiFeO_3$ thin films annealed at 100 °C–650 °C. The results indicate that Bi and Fe cations are close to the stoichiometry of $BiFeO_3$, whereas the deficiency of O anions possibly plays a key role in contributing to the leakage current of 10^{-5} A/cm^2 in a wide range of applied voltage rather than the ferroelectric polarizations of $BiFeO_3$ thin films annealed at high temperature.

Keywords: $BiFeO_3$ thin films, off-stoichiometry, high temperature annealing, backscattering spectrometry

PACS: 79.77.+g, 77.84.–s, 25.60.Dz, 82.80.Yc **DOI:** 10.1088/1674-1056/27/4/047901

1. Introduction

In the last several decades, it is well known that perovskite-multiferroic $BiFeO_3$ material has aroused a great deal of interest due to its remarkable coupling behavior of ferroelastic, ferroelectric, and ferromagnetic properties.[1–5] Pure rhombohedron phase $BiFeO_3$ exhibits antiferromagnetic nature at about 380 °C and ferroelectric behavior up to 810 °C,[6–8] which led to an inevitable research upsurge on phase transition theory involving ferromagnetic and ferroelectric ordering simultaneously.[9–11] These experimental and theoretical investigations would quicken the practical applications of multiferroic materials such as ferroelectric photovoltaic devices,[12,13] high- performace nanocapacitor,[14] and composite nanofibers.[15,16]

The physical properties of $BiFeO_3$ strongly depend on its own textures including the stoichiometry, impurities as well as other defect distributions. It is found that a significant number of research communities have developed various synthesis routes to prepare the perovskite structural $BiFeO_3$, although it is not easy to obtain in the sense of high-quality yield. Using the solid-state reaction method can prepare the pure phase $BiFeO_3$ ceramic, showing that it is an excellent ferroelectricity after the primary impurity phase of $Bi_2Fe_{2.75}$ has been leached with dilute nitric acid.[6] Palkar *et al.* proposed that the oxygen stoichiometry was critical to influence the variation of Fe ionic state in $BiFeO_3$ film fabricated by pulsed-laser deposition technique, which resulted in high conductivity of the film at room temperature.[17] The controversies on the leakage current mechanism of $BiFeO_3$-based heterostructures also focused on the stoichiometries of cations and anions in $BiFeO_3$ thin films fabricated by other epitaxial grown methods. It was reported that Bi-excess and Fe-excess in $BiFeO_3$ thin films induced a structural change from monoclinic to rhombohedral and formed the pyrochlore $Bi_2Fe_4O_9$ as well as γ-Fe_2O_3,[18] respectively. Due to a high thermal stability and slow rate of decomposition of Bi-precursor, single phase $BiFeO_3$ film growth was difficult to attain the reproducible mass-transfer in the process of metal organic chemical vapor deposition.[19] Nuclear resonance scattering reaction on $^{16}O(\alpha,\alpha)^{16}O$ at 3.045 MeV was employed to quantify the oxygen concentration in $BiFeO_3$ thin film, and the contribution of oxygen concentration to the leakage current was discussed by Yang, *et al.*[20] Therefore, the off-stoichiometry or nonstoichiometry effect on $BiFeO_3$ thin film has been further amplified in order to explain the physical properties observed in a certain range of temperature.

Compared with the high-cost epitaxial growth method, the sol–gel or hydrothermal synthesis route is one of the most popular methods to prepare $BiFeO_3$, which can be achieved

*Project supported by the National Natural Science Foundation of China (Grant Nos. 11605103, 11405117, and 11747074), the Guangdong Provincial Natural Science Foundation, China (Grant Nos. 2014A030307008 and 2016A030313670), and the Guangdong Provincial Science and Technology Planning Project, China (Grant Nos. 2016A010103041 and 2017A010103025).

†Corresponding author. E-mail: zswang@lingnan.edu.cn

© 2018 Chinese Physical Society and IOP Publishing Ltd

massively in liquid phase at low cost.[21–23] Combined with the film prepared by the spin coating technique, $BiFeO_3$ thin film can be fabricated on the surface of the substrate. Subsequent thermal treatment should be carried out for crystallization of $BiFeO_3$ film. The film stoichiometry on the substrate can also be analyzed by x-ray diffraction (XRD), x-ray photoelectron spectrum (XPS), energy dispersive spectrum (EDS), and other characterization methods.

Rutherford backscattering spectrometry (RBS) on the basis of energy-tunable particle accelerator apparatus, as a non-destructive detection for elemental composition, depth profile, and surface impurities in thin film, is widely used for ion beam material analysis.[24] Dedon *et al*. have taken full advantage of RBS to probe the role of stoichiometry, which can have an influence on the crystal and domain structures and properties of $BiFeO_3$ thin films systematically.[25] Along with ion beam channeling technology, RBS/channeling measurement can locate the interstitial atoms and other defects, in particular for doped rare-earth elements in $BiFeO_3$ films.[26]

In this paper, the sol–gel method is utilized to prepare colloidal sol that can be spin-coated onto the surface of the silicon matrix to form $BiFeO_3$ thin film with a thickness of several hundred nanometers. Next, the coated samples are subject to appropriate annealing schemes consisting of layer-by-layer annealing at 350 °C and final annealing at a temperature of 500 °C–650 °C. Eventually, the structure, stoichiometry, and physical properties of $BiFeO_3$ thin film on the silicon are characterized by XRD, RBS, scanning electron microscopy (SEM), and electrical measurement system. In order to quantitatively evaluate film stoichiometry, simulation software SIMNRA 6.05 is used for fitting experimental results. In light of these cases, it is likely to give us a guidance for optimizing the experimental preparation details and exploring a straightforward synthesis route to prepare the pure phase $BiFeO_3$ thin films.

2. Experimental details

The flow diagram of preparation details of $BiFeO_3$ thin films is displayed in Fig. 1(a). As the precursors, crystallized Fe $(NO_3)_3{\cdot}9H_2O$ and excess $Bi(NO_3)_3{\cdot}5H_2O$ (with excess of 5 wt%) were dissolved in the mixture of 5-ml glycol solution and 25-ml ethyl alcohol solution. Then 1-ml dilute nitric acid was put into the mixture solution, which can catalyze the hydrolyzation of metal salts. Next, magnetic stirring of the mixture was carried out for 1 h at a speed of 500 rpm/min. The 10-ml acetic anhydride was poured into the solution gradually while being stirred for at least 2 h. Finally, a sort of tan colloidal solution was not formed until the molarity was modulated to 0.2 M after adding suitable glycol and ethyl alcohol solutions. In the coming 5 to 7 days, the colloidal solution stood in an airtight beaker. The following step was spin coating of the solution onto the surface of n-type (100) Si substrate at a size of 10 mm×10 mm, which had been cleaned ultrasonically 3 times with ethyl alcohol and deionized water alternately. The speed of spin coater (KW-4A) was controlled at 4000 rpm/min for 30 s. After spin coating, all the samples were directly baked in an oven, keeping the temperature at 100 °C for 5 min. Then they were put into a furnace to pre-anneal them at 350 °C for 5 min in the atmosphere. With regard to thin films synthesized at several hundred nanometers, it was necessary to repeat the spin coating process for pre-annealing samples 10–20 times. The last annealing program was set to range from 500 °C to 650 °C in the atmosphere, for a dwelling time of 10 min.

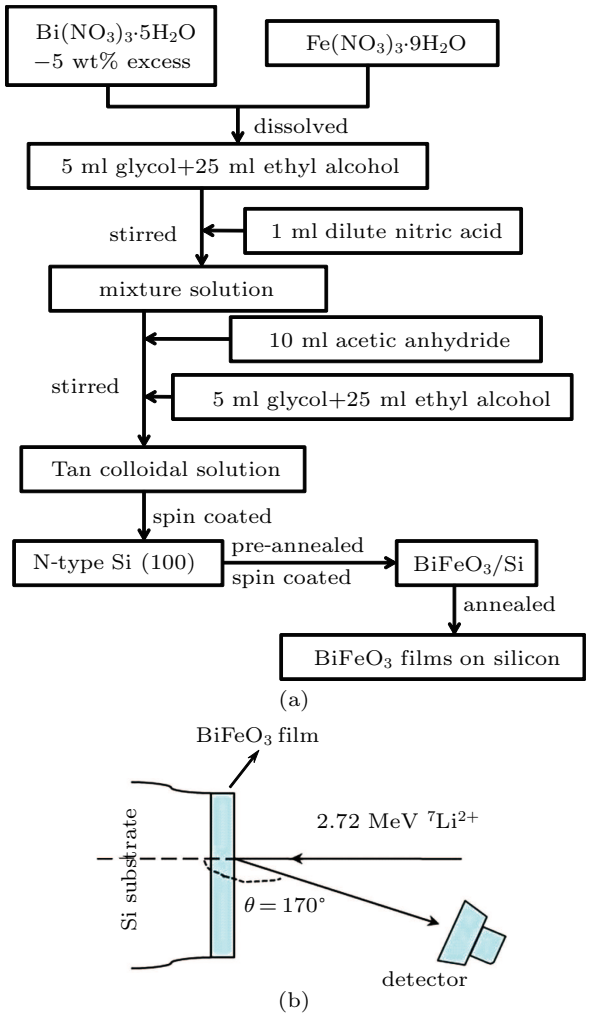


Fig. 1. (color online) (a) Flow diagram of details of preparing $BiFeO_3$ thin films, and (b) schematic diagram of detection geometry in the target chamber for ion beam analysis.

The XRD data were acquired using a standard diffractometer (D8 advanced) with Cu K_α radiation in steps of 0.4°/min in a range of θ–2θ at $10^\circ \sim 70^\circ$. The surface and cross-sectional morphologies were imaged by Sirion FEG SEM with attachment EDAX genesis 7000 EDS. Ion beam analysis was implemented on a 2×1.7 MV tandetron accelerator (GIC4117) using $^7Li^{2+}$ ions as projectiles at an initial

energy of 2.72 MeV. The schematic diagram of detection geometry in the target chamber is illustrated in Fig. 1(b). The ion beam current was 3 nA impinging onto the target perpendicularly, and the circular spot diameter was 1.5 mm. A passivated implanted planar silicon (PIPS, CANBERRA) detector with a resolution of 15 keV was mounted at a backscattering angle of 170° to collect backscattered ions. A beam integrator was used to monitor the ion current and record the total incident charge numbers. The vacuum was kept at about 10^{-5} Pa in the target chamber. The $BiFeO_3$ films annealed at 550 °C and 600 °C were made into heterostructures for leakage current measurement at an applied voltage of 30 V, and ferroelectric measurement using a ferroelectric tester (Radiant Technologies) at an applied voltage of 12 V at 1 kHz.

3. Results and discussion

Figure 2 depicts XRD patterns of $BiFeO_3$ thin films on silicon annealed at 500 °C–650 °C in steps of 50 °C after layer-by-layer pre-annealing at 350 °C. It is observed that all the thin films belong with polycrystalline rhombohedral perovskite structure whose lattice parameters are $a = b = 5.576$ Å, $c = 6.919$ Å, affiliated to the $R3c$ space group. There are impurity phase peaks centered at about 29° which are assigned to $Bi_2Fe_4O_9$, appearing at 500 °C, 550 °C, and 650 °C. But almost no impurity phase is observed at 600 °C, which is nearly in agreement with XRD results in Ref. [27]. This implies that the pure phase $BiFeO_3$ thin film can be obtained when annealing temperature is optimized at 600 °C.

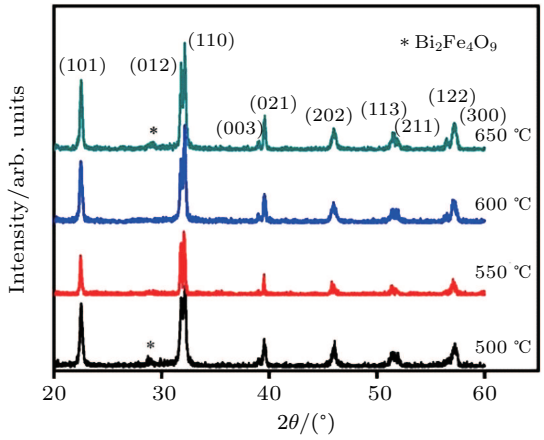


Fig. 2. (color online) XRD patterns of $BiFeO_3$ thin films annealed at 500 °C–650 °C.

In order to detect the surface morphology and thickness of $BiFeO_3$ thin film on the silicon substrate, two samples annealed at 500 °C and 600 °C were imaged as shown in Fig. 3. It is evident that $BiFeO_3$ thin films on the surface of silicon substrate are rather uniform, in spite of a number of porous structures that cannot contribute to densification of thin films. Fortunately, figures 3(c) and 3(d) indicate that there are less cavities in the samples annealed at 500 °C and 600 °C than in the sample annealed at 500 °C, and the interface between thin film and substrate is more unambiguous with a thickness of 298 nm (arrowed) of $BiFeO_3$ thin film annealed at 600 °C.

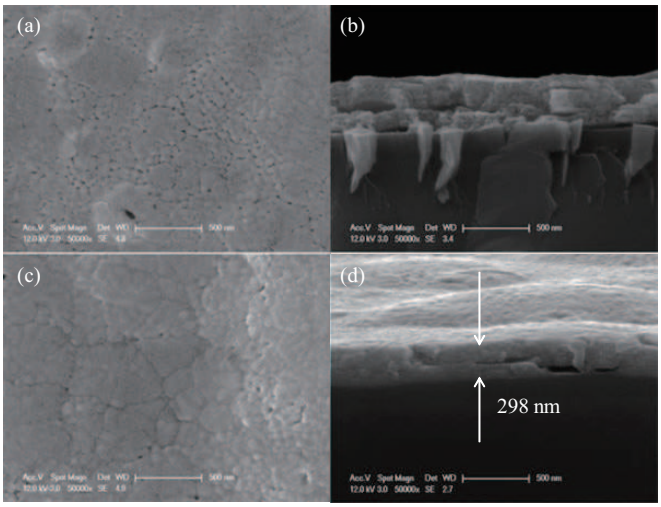


Fig. 3. Surface morphological and cross-sectional SEM images of $BiFeO_3$/Si annealed at ((a) and (b)) 500 °C and ((c) and (d)) 600 °C, respectively.

Figure 4 shows RBS spectra of the samples at room temperature (RT) and 100 °C–650 °C. Three main chemical elemental peaks in thin films are visualized while the signal peaks from silicon substrates can also be observed clearly. It is found that $BiFeO_3$ films without thermal treatment and only with baking in the oven at 100 °C have much larger thickness values than those of films annealed at high temperature, which can be inferred from the back-edge positions of Bi peaks. The RT spectrum indicates that the massive interstitials are present in the film without lattice restoration because the back edges of Bi-peak and Fe-peak have been severely broadened. Once the sample is annealed, the broadened back edge disappears.

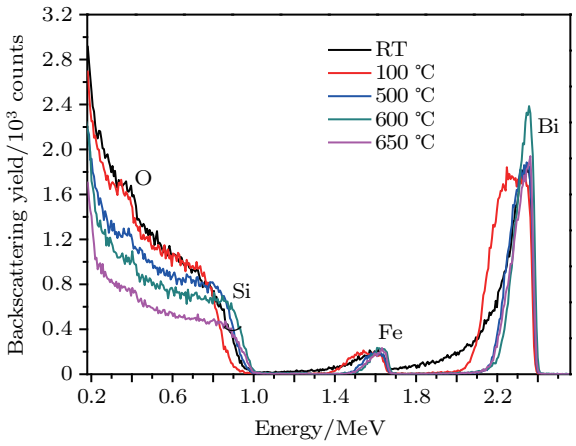


Fig. 4. (color online) RBS spectra of the samples at room temperature and different temperatures ranging from 100 °C to 650 °C.

Here, we have used the SIMNRA code to fit the experimental results of thin films annealed at 100 °C–650 °C so that film stoichiometry can be estimated quantificationally as shown in Fig. 5. The corresponding atomic concentration percentages in the films are recited in Table 1 and most depth pro-

files of atoms are detailed elsewhere.[28] The results from fitting data reveal that the thickness of $BiFeO_3$ thin film annealed at 100 °C is almost twice as large as at high temperature, but has more impurities. Especially, when the annealing temperature is over 100 °C, the exhaust of an excess of O content in the form of nitrogen-containing molecules and carbon dioxide that has escaped from thin films, makes it possible that the atomic ratio of Bi, Fe, and O is approximately 1:1:3 at 600 °C. We use a layer-by-layer annealing technique at 350 °C and successive spin coating process 10–20 times to compensate for the volatilization of Bi cations at high temperature, whereas O anions still decrease from 45.37 at.% to 16.61 at.% with the rise of temperature. It is possible to evaporate the organics and decomposition of nitrogen-containing organics below 200 °C, to release the carbon dioxide at 300 °C–450 °C, and to form the phase-crystallization step at 450 °C–600 °C with tiny weight loss, which can be responsible for the weight losses in films, summarized systematically by Xu *et al.*[21] The quantitative analyses of $BiFeO_3$ thin films on silicon annealed in a range of 100 °C–600 °C consistent with the results from their proposals. When annealing temperature is as high as 650 °C, oxygen deficiency is very visible to deviate from the theoretical stoichiometry of perovskite $BiFeO_3$. With respect to the content variations of Si and impurities, it should be detailed in the next discussion. So far, an optimized final annealing temperature is 600 °C, derived from XRD, SEM, and RBS results.

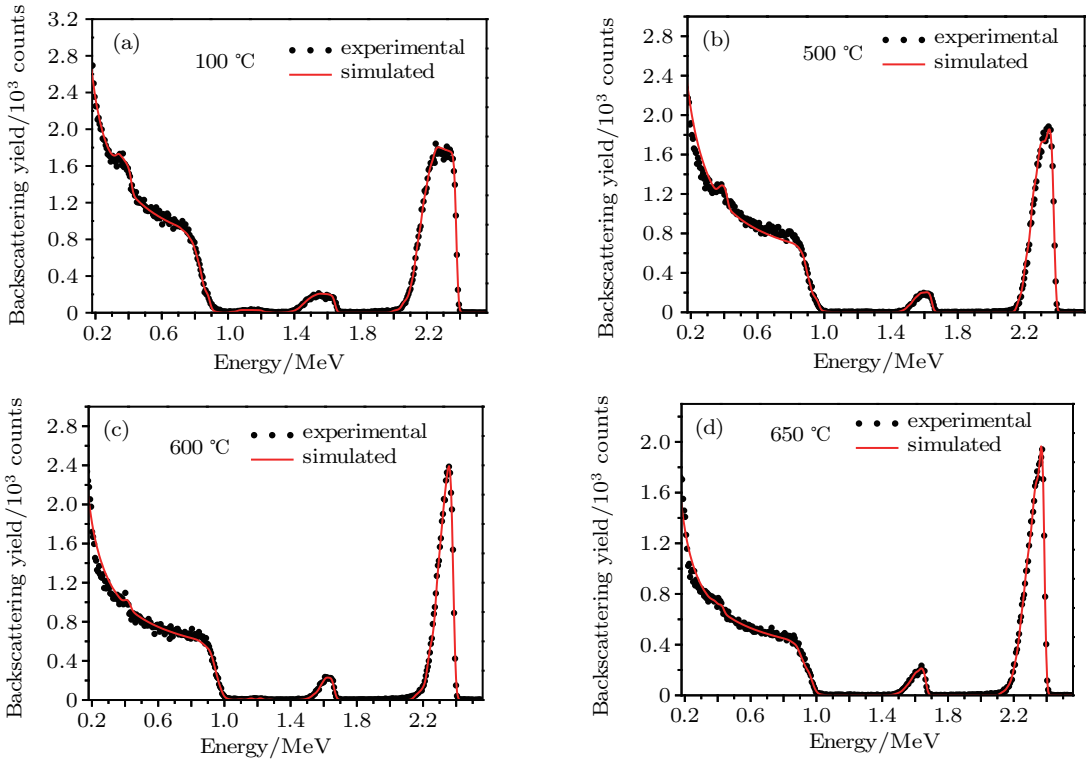


Fig. 5. (color online) Experimental and simulated RBS spectra of $BiFeO_3$ thin films under annealing temperatures of (a) 100 °C, (b) 500 °C, (c) 600 °C, and (d) 650 °C.

Table 1. Fitting results from SIMNRA simulation software.

Concentration/at.%	Bi	Fe	O	Si	Other	Sum/(atoms/cm^2)
100 °C	4.15	4.17	45.37	27.41	18.90	2.13×10^{18}
500 °C	5.99	5.80	31.27	50.37	6.57	1.15×10^{18}
600 °C	7.04	6.70	21.09	62.36	2.81	1.10×10^{18}
650 °C	7.92	8.05	16.61	66.68	0.74	1.23×10^{18}

Figures 6(a) and 6(b) show the current density–electric field (C–E) characteristics and ferroelectric polarization–electric field (P–E) hysteresis loops measured at room temperature for $BiFeO_3$ thin films annealed at 550 °C and 600 °C, respectively. It is observed from Fig. 6(a) that the surface leakage current density is 10^{-6} A/cm^{-2}–10^{-5} A/cm^2 in a wide range of applied electric fields, which reveals that $BiFeO_3$ thin films annealed at high temperature are eligible for heterostructures, even the leakage current is as low as 10^{-6} A/cm^2 at a low applied voltage of 5 V, as compared with those of 10^{-9} A/cm^2 of single-crystal $BiFeO_3$ bulk[29] and 10^{-7} A/cm^2 of $BiFeO_3$ thin film.[18,25] Figure 6(b) shows the relation of polarization as a function of applied electric field, and the spontaneous polarization (P_s) and remnant polarization (P_r) are approximately 7.09 μC/cm^2 and 4.63 μC/cm^2, the corresponding coercive electric field is about 103 kV/cm for the sample annealed at 550 °C. The performance of high conductive thin film annealed at 600 °C is worse with a P_s of 3.82 μC/cm^2 and a P_r of 2.24 μC/cm^2. It is supposed that the lack of a bottom electrode is a decisive factor that results in much weaker ferroelectric behavior.[30] However, we design the initial RBS characteri-

zation of $BiFeO_3$ thin film for introducing as few as possible chemical elements so that their concentrations can be determined accurately. Therefore, such $BiFeO_3$ thin films on silicon are available. Actually, oxygen deficiency in thin film induces a large number of vacancies to contribute to the leakage current mechanism rather than the increase of polarization.[17] We attempt to adopt a layer-by-layer annealing and continuous spin coating technique to compensate for the volatilization of Bi, but the O anions cannot be prevented from decreasing effectively during high temperature annealing. Due to the fact that the leakage current mechanism is not a predominating factor for the ferroelectric polarizing of multiferroic materials, the O deficiency is extremely critical for leakage current instead of polarization.

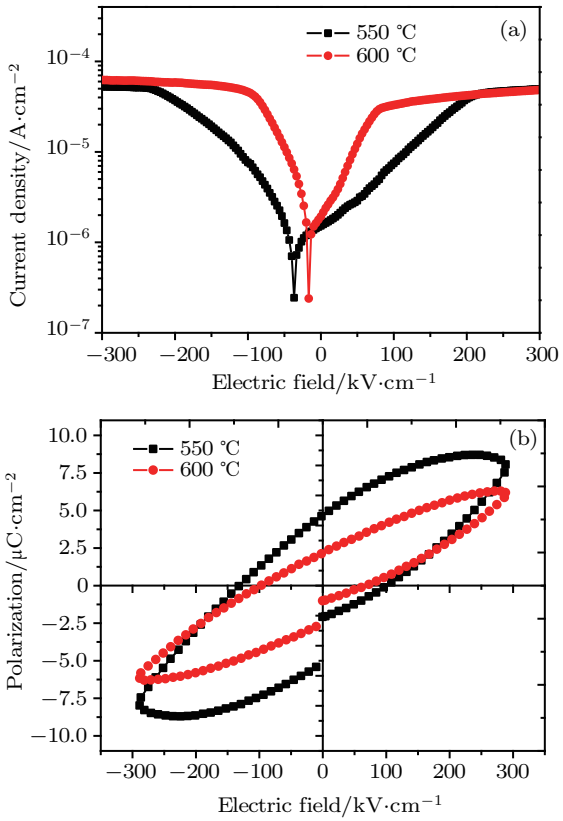


Fig. 6. (color online) (a) Room temperature *C*–*V* characteristics and (b) ferroelectric P–E hysteresis loops of $BiFeO_3$ thin films annealed at 550 °C and 600 °C.

It is counterintuitive that the impurities existing in $BiFeO_3$ thin films are not only $Bi_2Fe_4O_9$, labeled in Fig. 2, because of the sorts of nitrates or carbonates that are probably going to be introduced into thin films synthesized using the sol–gel method. Fortunately, these nitrogen-containing or carbon-containing compounds are mostly disintegrated to create oxynitride or carbon dioxide during high-temperature annealing, which is likely to be dedicated to the weight loss of thin film in accordance with RBS results.

It should be pointed out that the RBS characterization using Li^{2+} ions as the incident beam is not sensitive enough to light the nucleus, such as C, N, and O, but can improve the mass resolution of the heavy nucleus, especially for larger mass separations in a multi-component target.[31] When Li^{2+} ions are selected as incident ion beams, kinematic factors of the interactions with ^{12}C, ^{14}N, and ^{16}O are about 0.07, 0.11, and 0.15 at a backscattering angle of 170°,[17] so their scattering cross sections will overlap seriously into a signal peak of Si substrate in the low-energy region of the RBS spectrum. Therefore, the fitting data of O concentrations are not so accurate as Bi and Fe concentrations in Table 1. Because most of $BiFeO_3$ thin films have O-deficiency, resulting in a mass of O vacancies contributing to leakage current, which has been studied extensively in the literature. To some extent, O deficiency in $BiFeO_3$ thin film annealed at high temperature is considered as a paramount factor for leakage current. In turn, the accurate detecting of O concentrations in $BiFeO_3$ thin films must employ more sensitive characteristic methods, such as $^{16}O(\alpha,\alpha)^{16}O$ at 3.045 MeV and $^{15}O(P,\gamma)^{16}O$ at 3.4 MeV indirectly.[24] With the improvement of annealing temperature, the Si content in thin film increases dramatically as listed in Table 1. This means that the atomic diffusion occurring on the interface between thin film and Si substrate is extremely intense during high temperature annealing. The influences on electrical and magnetic properties of $BiFeO_3$ thin film due to the interfacial diffusion of Si atoms at high temperature have been corroborated and discussed systematically in our previous work.[28,32]

As is well known, there are some factors to determine the leakage current mechanism of $BiFeO_3$ thin film, such as the nonstoichiometry,[18,20,33] the thickness,[34,35] the impurity,[6,19] the matrix,[26,30] annealing schemes and microstructure.[36] In our work, it is speculated from MeV-ion backscattering spectrometry that using layer-by-layer annealing can make the ratio of Bi to Fe approach to 1:1 of off-stoichiometry film and can also produce few impurities, but O deficiency is still predominant inducing a large leakage current over 600 °C. The annealing temperature is as high as 500 °C exerted on the thin film at a thickness of 300 nm, which seems to degrade the resistance, because annealing temperature below 450 °C has been suggested for $BiFeO_3$ thin film prepared by the chemical solution method.[21] Selecting Si wafer as the deposition matrix is feasible, but it is probably going to lead to interfacial atomic diffusion at high temperature that may weaken the physical properties of $BiFeO_3$ thin film, and the lattice mismatch between $BiFeO_3$ and Si substrate has to be taken into consideration. In addition, the bottom electrode, the buffer layer of metallic oxides and rare-earth element doping in thin film can reduce the leakage current obviously.[26,30,35,37] Further studies on these aspects will pave the way to the improvement of the ferroelectric property of $BiFeO_3$ thin film prepared by the sol–gel method with the help of the layer-by-layer annealing technique.

4. Conclusions

We prepare $BiFeO_3$thin films with off-stoichiometry by the sol–gel method combined with a layer-by-layer annealing technique, and O deficiencies and impurities in thin films are leading factors to have an influence on the physical properties. The XRD patterns indicate that the primary impurity phase is $Bi_2Fe_4O_9$ and few amorphous inorganic salts, and pure phase $BiFeO_3$ is attained in the condition of annealing temperature at 600 °C. The quantitative results of off-stoichiometry films are figured out by RBS fitting program SIMNRA 6.05, which explains the weight losses of the samples annealed from 100 °C to 650 °C by performing the reductions of total atomic numbers in thin films. The layer-by-layer annealing scheme can compensate for the exhausts of Bi and Fe cations instead of O anions at high temperature, which is possible to induce a leakage current as high as 10^{-5} A/cm^2 in a wide range of applied voltage instead of ferroelectric polarization features of $BiFeO_3$ thin films annealed at high temperature.

References

[1] Wang J, Neaton J B, Zheng H, Nagarajan V, Ogale S B, Liu B, Viehland D, Vaithyanathan V, Schlom D G, Waghmare U V, Spaldin N A, Rabe K M, Wuttig M and Ramesh R 2003 *Science* **299** 1719

[2] Hur N, Park S, Sharma P A, Ahn J S, Guha S and Cheong S W 2004 *Nature* **429** 392

[3] Zhao T, Scholl A, Zavaliche F, Lee K, Barry M, Doran A, Cruz M P, Chu Y H, Ederer C, Spaldin N A, Das R R, Kim D M, Baek S H, Eom C B and Ramesh R 2006 *Nat. Mater.* **5** 823

[4] Wojdel J C and Íñiguez J 2009 *Phys. Rev. Lett.* **103** 267205

[5] Ju C, Yang J C. Luo C, Shafer P, Liu H J, Huang Y L, Kuo H H, Xue F, Luo C W, He Q, Yu P, Arenholz E, Chen L Q, Zhu J, Lu X and Chu Y H 2016 *Adv. Mater.* **28** 876

[6] Mahesh Kumar M, Palkar V R, Srinivas K and Suryanarayana S V 2000 *Appl. Phys. Lett.* **76** 2764

[7] Kim J K, Kim S S and Kim W J 2005 *Mater. Lett.* **59** 4006

[8] Hyun S W, Choi K R and Kim C S 2010 *J. Supercond. Nov. Magn.* **24** 635

[9] Guennou M, Bouvier P, Chen G S, Dkhil B, Haumont R, Garbarino G and Kreisel J 2011 *Phys. Rev. B.* **84** 174107

[10] Infante C, Juraszek J, Fusi l S, Dupe B, Gemeiner P, Diéguez O, Pailloux F, Jouen S, Jacquet E, Geneste G, Pacaud J, I'ñiguez J, Bellaiche L, Barthélémy A, Dkhil B and Bibes M 2011 *Phys. Rev. Lett.* **107** 237601

[11] Volkova L M and Marinin D V 2011 *J. Supercond. Nov. Magn.* **24** 2161

[12] Moniz S J A, Quesada-Cabrera R, Blackman C S, Tang J, Southern P, Weaver P M and Carmalt C J 2014 *J. Mater. Chem.* **2** 2922

[13] Fei L, Hu Y, Li X, Song R, Sun L, Huang H, Gu H, Chan H L W and Wang Y 2015 *ACS Appl. Mater. Interfaces* **7** 3665

[14] Zhao L, Lu Z, Zhang F, Tian G, Song X, Li Z, Huang K, Zhang Z, Qin M, Wu S, Lu X, Zeng M, Gao X, Dai J and Liu J M 2015 *Sci. Rep.* **5** 9680

[15] Xu Q, Sobhan M, Anariba F, Ho J W C, Chen Z and Wu P 2014 *Phys. Chem. Chem. Phys.* **16** 23089

[16] Sobhan M, Xu Q, Katoch A, Anariba F, Kim S S and Wu P 2015 *Nanotechnol.* **26** 175501

[17] Palkar V R, John J and Pinto R 2002 *Appl. Phys. Lett.* **80** 1628

[18] Lahmar A, Zhao K, Habouti S, Dietze M, Solterbeck C H and Es-Souni M 2011 *Solid State Ionics* **202** 1

[19] kartavtseva M S, Gorbenko O Yu, Kaul A R, Fusil S, Barthélémy A and Bouzehouane K 2008 *Ferroelectrics* **374** 20

[20] Yang H, Wang Y Q, Wang H and Jia Q X 2010 *Appl. Phys. Lett.* **96** 012909

[21] Xu J H, Ke H, Jia D C, Wang W and Zhou Y 2009 *J. Alloys Compd.* **472** 473

[22] Yang X, Zhang Y, Xu G, Wei X, Ren Z, Shen G and Han G 2013 *Mater. Res. Bull.* **48** 1694

[23] Zhang Q, Nagarajan V and Standard O 2014 *J. Appl. Phys.* **116** 066810

[24] Wang Y Q and Nastasi M 2009 *Handbook of modern ion beam materials analysis*, 2nd edn. (Warrendale: Materials Research Society) pp. 65–92

[25] Dedon Liv R, Saremi S, Chen Z H, Damodaran Anoop R, Apgar Brent A, Gao R and Martin Lane W 2016 *Chem. Mater.* **28** 5952

[26] Lazenka V V, Lorenz M, Modarresi H, Brachwitz K, Schwinkendorf P, Böntgen T, Vanacken J, Ziese M, Grundmann M and Moshchalkov V V 2013 *J. Phys. D: Appl. Phys.* **46** 175006

[27] Carvalho T T and Tavares P B 2008 *Mater. Lett.* **62** 3984

[28] Xiao R Z, Zhang Z D, Pelenovich V O, Wang Z S, Zhang R, Li H, Liu Y, Huang Z H and Fu D J 2014 *Chin. Phys. B* **23** 077504

[29] Catalan G and Scott J F 2009 *Adv. Mater.* **21** 2463

[30] Zhang Q, Sando D and Nagarajan V 2016 *J. Mater. Chem. C* **4** 4092

[31] Chu W K, Mayer J W and Nicolet M A 1978 *Backscattering spectrometry* (New York : Academic Press) pp. 57–59

[32] Xiao R Z, Wang Z S, Yuan X B, Zhou J J. Mao Z L, Su H S, Li B and Fu D J 2016 *Nul. Instrum. Mathod Phys. Res. B* **384** 106

[33] Ito T, Ushiyama T, Aoki M, Tomioka Y, Hakuta Y, Takashima H and Wang R 2013 *Inorg. Chem.* **52** 12806

[34] Liu G and Nan C W 2005 *J. Phys. D: Appl. Phys.* **38** 584

[35] Yakovlev S, Zekonyte J, Solterbeck C H and Es-Souni M 2005 *Thin Solid Films* **493** 24

[36] Iakovlev S, Solterbeck C H, Kuhnke M and Es-Souni M 2005 *J. Appl. Phys.* **97** 094901

[37] Huang A and Shannigrahi S R 2011 *J. Alloys Compd.* **509** 2054